

University of Nebraska - Lincoln

DigitalCommons@University of Nebraska - Lincoln

Mechanical & Materials Engineering Faculty
Publications

Mechanical & Materials Engineering, Department
of

2017

Effects of aspect ratio on the mode couplings of thin-film bulk acoustic wave resonators

Nian Li

Nanjing University of Aeronautics and Astronautics


Zhenghua Qian

University of Nebraska-Lincoln, qianzh@nuaa.edu.cn

Jiashi Yang

University of Nebraska-Lincoln, jyang1@unl.edu

Follow this and additional works at: <http://digitalcommons.unl.edu/mechengfacpub>

 Part of the [Mechanics of Materials Commons](#), [Nanoscience and Nanotechnology Commons](#), [Other Engineering Science and Materials Commons](#), and the [Other Mechanical Engineering Commons](#)

Li, Nian; Qian, Zhenghua; and Yang, Jiashi, "Effects of aspect ratio on the mode couplings of thin-film bulk acoustic wave resonators" (2017). *Mechanical & Materials Engineering Faculty Publications*. 271.

<http://digitalcommons.unl.edu/mechengfacpub/271>

This Article is brought to you for free and open access by the Mechanical & Materials Engineering, Department of at DigitalCommons@University of Nebraska - Lincoln. It has been accepted for inclusion in Mechanical & Materials Engineering Faculty Publications by an authorized administrator of DigitalCommons@University of Nebraska - Lincoln.

Effects of aspect ratio on the mode couplings of thin-film bulk acoustic wave resonators

Nian Li,¹ Zhenghua Qian,^{2,a} and Jiashi Yang^{2,b}

¹State Key Laboratory of Mechanics and Control of Mechanical Structures, College of Aerospace Engineering, Nanjing University of Aeronautics and Astronautics, Nanjing 210016, China

²Department of Mechanical and Materials Engineering, The University of Nebraska-Lincoln, Lincoln, Nebraska 68588-0526, USA

(Received 23 March 2017; accepted 8 May 2017; published online 18 May 2017)

We studied mode couplings in thin film bulk acoustic wave resonators of a piezoelectric film on a dielectric layer operating with the fundamental thickness-extensional mode. A system of plate equations derived in our previous paper was used which includes the couplings to the unwanted in-plane extension, flexure, fundamental and second-order thickness shear modes. It was shown that the couplings depend strongly on the plate length/thickness ratio. For a relatively clean operating mode with weak couplings to unwanted modes, a series of discrete values of the plate length/thickness ratio should be avoided and these values were determined in the present paper. The results can be of great significance to the design and optimization of film bulk acoustic wave resonators. © 2017 Author(s). All article content, except where otherwise noted, is licensed under a Creative Commons Attribution (CC BY) license (<http://creativecommons.org/licenses/by/4.0/>). [<http://dx.doi.org/10.1063/1.4983890>]

I. INTRODUCTION

Acoustic wave resonators made from piezoelectric crystals are key components of electrical circuits called oscillators in a lot of electronic equipment.^{1,2} As frequency standards, resonators are widely used for time keeping, frequency operation, and signal generation and processing. Frequency shifts in resonators caused by various effects like a temperature change or stress are the foundation of resonator-based acoustic wave sensors. Conventional piezoelectric resonators are made from crystals like quartz and lithium niobate, etc. They may operate with bulk^{1,2} or surface acoustic waves.^{3,4} During the last couple of decades, researchers succeeded in depositing with good enough quality a thin piezoelectric film of AlN or ZnO on a silicon layer to form thin-film bulk acoustic wave resonators (FBARs or TFBARs) operating in the GHz frequency range.⁵⁻⁷ FBARs have several advantages over conventional crystal resonators.^{8,9} They have also been used to make acoustic wave sensors.^{10,11} Structurally, FBARs are multilayered plates with metal electrodes, a piezoelectric film, and an elastic layer. In this paper we study the most common FBARs in which the c-axis of the piezoelectric films are in the plate thickness direction and the FBARs operate with the fundamental thickness-extensional mode of the plates. There are other structural types of FBARs operating with shear modes¹²⁻¹⁶ or solidly mounted on an elastic substrate.^{17,18} Their modeling requires separate and fundamentally different efforts and is out of the scope of the present paper.

Because of the structural complexity and piezoelectric coupling, theoretical modeling of FBARs is very challenging mathematically. Typical theoretical models of FBARs are for the operating thickness-extensional mode only. The simplest models are one-dimensional,^{14,15,19,20} with onespatial

^a qianzh@nuaa.edu.cn

^b jyang1@unl.edu

variable along the normal direction of the plates only. One-dimensional models are valid for pure thickness-extensional modes which can exist in unbounded plates. With some approximation of the variation of the fields along the plate thickness, Tiersten and Stevens once derived a single two-dimensional scalar differential equation²¹ that can describe the in-plane variation of the operating thickness-extensional mode (transversely varying thickness-extensional mode). The scalar equation has been used in the analysis of a rectangular trapped energy resonator in Refs. 21 and 22, a two-port filter in Refs. 21 and 23, and a rectangular resonator with ring electrodes for sensor application.²⁴

In real applications, in addition to the operating thickness-extensional mode, other modes are often present in the operation of FBARs. These unwanted modes are called spurious modes.²⁵ They affect the performance of FBARs and are highly undesirable in general. For a successful device, we need to be able to describe and predict these spurious modes so that they can be avoided through proper design. However, the theoretical models used in Refs. 14, 15, and 19–24 for the thickness-extensional mode alone cannot treat the couplings between the operating mode and the spurious modes. Theoretical modeling of mode couplings in FBARs is crucial to the current design and manufacturing of FBARs.

In our previous paper,²⁶ a system of two-dimensional equations for the operating thickness-extensional mode with couplings to the relevant spurious modes was derived. The spurious modes included in Ref. 26 are the in-plane extensional mode, the flexural mode, the fundamental thickness-shear mode, and the second-order thickness-shear mode. These are the modes that are coupled to the operating thickness-extensional mode in the frequency range of interest of FBARs. In Ref. 26, the propagation of these coupled waves in unbounded plates was studied to verify the equations obtained and determine the correction factors in the equations. In this paper we use the equations obtained in Ref. 26 to analyze the couplings between the operating mode and the spurious modes in a finite plate FBAR.

II. GOVERNING EQUATIONS

Consider the four-layer plate in Fig. 1. The x_2 axis is determined from x_3 and x_1 by the right-hand rule. The x_1 and x_2 axes are in the middle plane of the plate. The total plate thickness is $2h = h^s + h'' + h^f + h'$. For a free vibration analysis, the electrodes are shorted and the electric field vanishes within the approximation of the plate theory.

We consider straight-crested modes with $u_2=0$ and $\partial/\partial x_2 = 0$. The plate theory in Ref. 26 which is to be used in this paper is summarized briefly below. The displacement field is approximated by

$$\begin{aligned} u_1 &\cong u_1^{(0)}(x_1, t) + u_1^{(1)}(x_1, t)x_3 + u_1^{(2)}(x_1, t)x_3^2, \\ u_3 &\cong u_3^{(0)}(x_1, t) + u_3^{(1)}(x_1, t)x_3, \end{aligned} \quad (1)$$

where $u_1^{(0)}$ is the in-plane extension, $u_1^{(1)}$ is the fundamental thickness shear, $u_1^{(2)}$ is the second-order thickness shear, $u_3^{(0)}$ is the flexure, and $u_3^{(1)}$ is the thickness extension. The relevant plate strains corresponding to Eq. (1) are

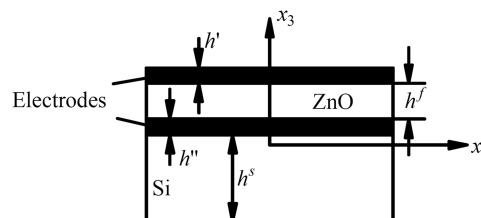


FIG. 1. A four-layer plate as an FBAR and the defined coordinate system.

$$\begin{aligned}
S_1^{(0)} &= u_{1,1}^{(0)}, & S_3^{(0)} &= u_3^{(1)}, & S_5^{(0)} &= u_{3,1}^{(0)} + u_1^{(1)}, \\
S_1^{(1)} &= u_{1,1}^{(1)}, & S_5^{(1)} &= u_{3,1}^{(1)} + 2u_1^{(2)}, \\
S_1^{(2)} &= u_{1,1}^{(2)},
\end{aligned} \tag{2}$$

The equations of motion for $u_1^{(0)}$, $u_1^{(1)}$, $u_1^{(2)}$, $u_3^{(0)}$ and $u_3^{(1)}$ are

$$\begin{aligned}
T_{11,1}^{(0)} &= \rho^{(0)}\ddot{u}_1^{(0)} + \rho^{(1)}\ddot{u}_1^{(1)} + \rho^{(2)}\ddot{u}_1^{(2)}, \\
T_{13,1}^{(0)} &= \rho^{(0)}\ddot{u}_3^{(0)} + \rho^{(1)}\kappa_3\ddot{u}_3^{(1)}, \\
T_{11,1}^{(1)} - T_{31}^{(0)} &= \rho^{(1)}\ddot{u}_1^{(0)} + \rho^{(2)}\ddot{u}_1^{(1)} + \rho^{(3)}\ddot{u}_1^{(2)}, \\
T_{13,1}^{(1)} - T_{33}^{(0)} &= \rho^{(1)}\ddot{u}_3^{(0)} + \rho^{(2)}\kappa_3^2\ddot{u}_3^{(1)}, \\
T_{11,1}^{(2)} - 2T_{31}^{(1)} &= \rho^{(2)}\ddot{u}_1^{(0)} + \rho^{(3)}\ddot{u}_1^{(1)} + \rho^{(4)}\ddot{u}_1^{(2)},
\end{aligned} \tag{3}$$

where the moments of the mass distribution along the plate thickness are defined by

$$\rho^{(n)} = \int_{-h}^h \rho x_3^n dx_3. \tag{4}$$

The resultants in Eq. (3) are related to the plate strains in Eq. (2) through the following plate constitutive relations:

$$\begin{aligned}
T_{11}^{(0)} &= c_{11}^{(0)}S_1^{(0)} + \kappa_1 c_{13}^{(0)}S_3^{(0)} + c_{11}^{(1)}S_1^{(1)} + c_{11}^{(2)}S_1^{(2)} \\
&\quad + c_{13}^{(2)}S_1^{(1)}\gamma_{3110} + c_{13}^{(4)}S_1^{(2)}\gamma_{3210} + c_{13}^{(1)}S_1^{(0)}\gamma_{3110} \\
&\quad + \kappa_1 c_{33}^{(1)}S_3^{(0)}\gamma_{3110} + c_{13}^{(2)}S_1^{(0)}\gamma_{3210} + \kappa_1 c_{33}^{(2)}S_3^{(0)}\gamma_{3210} + c_{13}^{(3)}S_1^{(1)}\gamma_{3210} + c_{13}^{(3)}S_1^{(2)}\gamma_{3110}, \\
T_{13}^{(0)} &= \kappa_0^2 c_{44}^{(0)}S_5^{(0)} + \kappa_0 \kappa_2 c_{44}^{(1)}S_5^{(1)} - \kappa_0^2 S_5^{(0)} \frac{c_{44}^{(2)}c_{44}^{(2)}}{c_{44}^{(4)}} - \kappa_0 \kappa_2 S_5^{(1)} \frac{c_{44}^{(2)}c_{44}^{(3)}}{c_{44}^{(4)}}, \\
T_{11}^{(1)} &= c_{11}^{(1)}S_1^{(0)} + \kappa_1 c_{13}^{(1)}S_3^{(0)} + c_{11}^{(2)}S_1^{(1)} + c_{11}^{(3)}S_1^{(2)} \\
&\quad + c_{13}^{(2)}S_1^{(1)}\gamma_{3111} + c_{13}^{(4)}S_1^{(2)}\gamma_{3211} + c_{13}^{(1)}S_1^{(0)}\gamma_{3111} \\
&\quad + \kappa_1 c_{33}^{(1)}S_3^{(0)}\gamma_{3111} + c_{13}^{(2)}S_1^{(0)}\gamma_{3211} + \kappa_1 c_{33}^{(2)}S_3^{(0)}\gamma_{3211} + c_{13}^{(3)}S_1^{(1)}\gamma_{3211} + c_{13}^{(3)}S_1^{(2)}\gamma_{3111}, \\
T_{13}^{(1)} &= \kappa_0 \kappa_2 c_{44}^{(1)}S_5^{(0)} + \kappa_2^2 c_{44}^{(2)}S_5^{(1)} - \kappa_0 \kappa_2 S_5^{(0)} \frac{c_{44}^{(2)}c_{44}^{(3)}}{c_{44}^{(4)}} - \kappa_2^2 S_5^{(1)} \frac{c_{44}^{(3)}c_{44}^{(3)}}{c_{44}^{(4)}}, \\
T_{33}^{(0)} &= \kappa_1 c_{13}^{(0)}S_1^{(0)} + \kappa_1^2 c_{33}^{(0)}S_3^{(0)} + \kappa_1 c_{13}^{(1)}S_1^{(1)} + \kappa_1 c_{13}^{(2)}S_1^{(2)} + c_{13}^{(2)}S_1^{(1)}\kappa_1\gamma_{3130} \\
&\quad + c_{13}^{(4)}S_1^{(2)}\kappa_1\gamma_{3230} + c_{13}^{(1)}S_1^{(0)}\kappa_1\gamma_{3130} + \kappa_1^2 c_{33}^{(1)}S_3^{(0)}\gamma_{3130} + c_{13}^{(2)}S_1^{(0)}\kappa_1\gamma_{3230} \\
&\quad + \kappa_1^2 c_{33}^{(2)}S_3^{(0)}\gamma_{3230} + c_{13}^{(3)}S_1^{(1)}\kappa_1\gamma_{3230} + c_{13}^{(3)}S_1^{(2)}\kappa_1\gamma_{3130}, \\
T_{11}^{(2)} &= c_{11}^{(2)}S_1^{(0)} + \kappa_1 c_{13}^{(2)}S_3^{(0)} + c_{11}^{(3)}S_1^{(1)} + c_{11}^{(4)}S_1^{(2)} \\
&\quad + c_{13}^{(2)}S_1^{(1)}\gamma_{3112} + c_{13}^{(4)}S_1^{(2)}\gamma_{3212} + c_{13}^{(1)}S_1^{(0)}\gamma_{3112} \\
&\quad + \kappa_1 c_{33}^{(1)}S_3^{(0)}\gamma_{3112} + c_{13}^{(2)}S_1^{(0)}\gamma_{3212} + \kappa_1 c_{33}^{(2)}S_3^{(0)}\gamma_{3212} + c_{13}^{(3)}S_1^{(1)}\gamma_{3212} + c_{13}^{(3)}S_1^{(2)}\gamma_{3112},
\end{aligned} \tag{5}$$

where

$$c_{pq}^{(n)} = \int_{-h}^h c_{pq} x_3^n dx_3, \tag{6}$$

and c_{pq} are the usual elastic constants. In Eq. (5), we have denoted

$$\begin{aligned}
\gamma_{3110} &= \frac{c_{33}^{(3)}c_{13}^{(2)} - c_{33}^{(4)}c_{13}^{(1)}}{c_{33}^{(2)}c_{33}^{(4)} - c_{33}^{(3)}c_{33}^{(3)}}, & \gamma_{3130} &= \frac{c_{33}^{(3)}c_{33}^{(2)} - c_{33}^{(4)}c_{33}^{(1)}}{c_{33}^{(2)}c_{33}^{(4)} - c_{33}^{(3)}c_{33}^{(3)}}, \\
\gamma_{3111} &= \frac{c_{33}^{(3)}c_{13}^{(3)} - c_{33}^{(4)}c_{13}^{(2)}}{c_{33}^{(2)}c_{33}^{(4)} - c_{33}^{(3)}c_{33}^{(3)}}, & \gamma_{3112} &= \frac{c_{33}^{(3)}c_{13}^{(4)} - c_{33}^{(4)}c_{13}^{(3)}}{c_{33}^{(2)}c_{33}^{(4)} - c_{33}^{(3)}c_{33}^{(3)}}, \\
\gamma_{3210} &= \frac{c_{33}^{(3)}c_{13}^{(1)} - c_{33}^{(2)}c_{13}^{(2)}}{c_{33}^{(2)}c_{33}^{(4)} - c_{33}^{(3)}c_{33}^{(3)}}, & \gamma_{3230} &= \frac{c_{33}^{(3)}c_{33}^{(1)} - c_{33}^{(2)}c_{33}^{(2)}}{c_{33}^{(2)}c_{33}^{(4)} - c_{33}^{(3)}c_{33}^{(3)}}, \\
\gamma_{3211} &= \frac{c_{33}^{(3)}c_{13}^{(2)} - c_{33}^{(2)}c_{13}^{(3)}}{c_{33}^{(2)}c_{33}^{(4)} - c_{33}^{(3)}c_{33}^{(3)}}, & \gamma_{3212} &= \frac{c_{33}^{(3)}c_{13}^{(3)} - c_{33}^{(2)}c_{13}^{(4)}}{c_{33}^{(2)}c_{33}^{(4)} - c_{33}^{(3)}c_{33}^{(3)}}.
\end{aligned} \tag{7}$$

$\kappa_0, \kappa_1, \kappa_2$ and κ_3 are correction factors²⁶ whose values will be given later. With successive substitutions from Eqs. (2) and (5), we can write Eq. (3) as five equations for $u_1^{(0)}, u_1^{(1)}, u_1^{(2)}, u_3^{(0)}$ and $u_3^{(1)}$:

$$\begin{aligned}
& \left[c_{11}^{(0)} + c_{13}^{(1)}\gamma_{3110} + c_{13}^{(2)}\gamma_{3210} \right] u_{1,11}^{(0)} + \left[c_{11}^{(1)} + c_{13}^{(2)}\gamma_{3110} + c_{13}^{(3)}\gamma_{3210} \right] u_{1,11}^{(1)} \\
& + \left[\kappa_1 c_{13}^{(0)} + \kappa_1 c_{33}^{(2)}\gamma_{3210} + \kappa_1 c_{33}^{(1)}\gamma_{3110} \right] u_{3,1}^{(1)} + \left[c_{11}^{(2)} + c_{13}^{(4)}\gamma_{3210} + c_{13}^{(3)}\gamma_{3110} \right] u_{1,11}^{(2)} \\
& = \rho^{(0)}\ddot{u}_1^{(0)} + \rho^{(1)}\ddot{u}_1^{(1)} + \rho^{(2)}\ddot{u}_1^{(2)},
\end{aligned} \tag{8}$$

$$\begin{aligned}
& \left[\kappa_0^2 c_{44}^{(0)} - \frac{\kappa_0 c_{44}^{(2)}}{c_{44}^{(4)}} \kappa_0 c_{44}^{(2)} \right] \left[u_{1,1}^{(1)} + u_{3,11}^{(0)} \right] + \left[\kappa_0 \kappa_2 c_{44}^{(1)} - \frac{\kappa_0 c_{44}^{(2)}}{c_{44}^{(4)}} \kappa_2 c_{44}^{(3)} \right] \left[u_{3,11}^{(1)} + 2u_{1,1}^{(2)} \right] \\
& = \rho^{(0)}\ddot{u}_3^{(0)} + \rho^{(1)}\kappa_3 \ddot{u}_3^{(1)},
\end{aligned} \tag{9}$$

$$\begin{aligned}
& \left[c_{11}^{(1)} + c_{13}^{(1)}\gamma_{3111} + c_{13}^{(2)}\gamma_{3211} \right] u_{1,11}^{(0)} + \left[c_{11}^{(2)} + c_{13}^{(2)}\gamma_{3111} + c_{13}^{(3)}\gamma_{3211} \right] u_{1,11}^{(1)} \\
& + \left[\kappa_1 c_{13}^{(1)} + \kappa_1 c_{33}^{(1)}\gamma_{3111} + \kappa_1 c_{33}^{(2)}\gamma_{3211} - \kappa_0 \kappa_2 c_{44}^{(1)} + \frac{\kappa_0 c_{44}^{(2)}}{c_{44}^{(4)}} \kappa_2 c_{44}^{(3)} \right] u_{3,1}^{(1)} \\
& + \left[c_{11}^{(3)} + c_{13}^{(4)}\gamma_{3211} + c_{13}^{(3)}\gamma_{3111} \right] u_{1,11}^{(2)} \\
& - \left[\kappa_0^2 c_{44}^{(0)} - \frac{\kappa_0 c_{44}^{(2)}}{c_{44}^{(4)}} \kappa_0 c_{44}^{(2)} \right] \left[u_{3,1}^{(0)} + u_1^{(1)} \right] - 2 \left[\kappa_0 \kappa_2 c_{44}^{(1)} - \frac{\kappa_0 c_{44}^{(2)}}{c_{44}^{(4)}} \kappa_2 c_{44}^{(3)} \right] u_1^{(2)} \\
& = \rho^{(1)}\ddot{u}_1^{(0)} + \rho^{(2)}\ddot{u}_1^{(1)} + \rho^{(3)}\ddot{u}_1^{(2)},
\end{aligned} \tag{10}$$

$$\begin{aligned}
& \left[\kappa_0 \kappa_2 c_{44}^{(1)} - \frac{\kappa_2 c_{44}^{(3)}}{c_{44}^{(4)}} \kappa_0 c_{44}^{(2)} \right] u_{3,11}^{(0)} + \left[\kappa_2^2 c_{44}^{(2)} - \frac{\kappa_2 c_{44}^{(3)}}{c_{44}^{(4)}} \kappa_2 c_{44}^{(3)} \right] u_{3,11}^{(1)} \\
& - \left[\kappa_1 c_{13}^{(0)} + \kappa_1 c_{13}^{(1)}\gamma_{3130} + \kappa_1 c_{13}^{(2)}\gamma_{3230} \right] u_{1,1}^{(0)} \\
& - \left[\kappa_1 c_{13}^{(1)} + \kappa_1 c_{13}^{(2)}\gamma_{3130} + \kappa_1 c_{13}^{(3)}\gamma_{3230} - \kappa_0 \kappa_2 c_{44}^{(1)} + \frac{\kappa_2 c_{44}^{(3)}}{c_{44}^{(4)}} \kappa_0 c_{44}^{(2)} \right] u_{1,1}^{(1)} \\
& - \left[\kappa_1^2 c_{33}^{(0)} + \kappa_1^2 c_{33}^{(1)}\gamma_{3130} + \kappa_1^2 c_{33}^{(2)}\gamma_{3230} \right] u_3^{(1)} \\
& - \left[\kappa_1 c_{13}^{(2)} + \kappa_1 c_{13}^{(4)}\gamma_{3230} + \kappa_1 c_{13}^{(3)}\gamma_{3130} - 2\kappa_2^2 c_{44}^{(2)} + 2\frac{\kappa_2 c_{44}^{(3)}}{c_{44}^{(4)}} \kappa_2 c_{44}^{(3)} \right] u_{1,1}^{(2)} \\
& = \rho^{(1)}\ddot{u}_3^{(0)} + \rho^{(2)}\kappa_3^2 \ddot{u}_3^{(1)},
\end{aligned} \tag{11}$$

$$\begin{aligned}
& \left[c_{11}^{(2)} + c_{13}^{(1)} \gamma_{3112} + c_{13}^{(2)} \gamma_{3212} \right] u_{1,11}^{(0)} + \left[c_{11}^{(3)} + c_{13}^{(2)} \gamma_{3112} + c_{13}^{(3)} \gamma_{3212} \right] u_{1,11}^{(1)} \\
& + \left[\kappa_1 c_{13}^{(2)} + \kappa_1 c_{33}^{(1)} \gamma_{3112} + \kappa_1 c_{33}^{(2)} \gamma_{3212} - 2\kappa_2 c_{44}^{(2)} + 2 \frac{\kappa_2 c_{44}^{(3)}}{c_{44}^{(4)}} \kappa_2 c_{44}^{(3)} \right] u_{3,1}^{(1)} \\
& + \left[c_{11}^{(4)} + c_{13}^{(4)} \gamma_{3212} + c_{13}^{(3)} \gamma_{3112} \right] u_{1,11}^{(2)} \\
& - 2 \left[\kappa_0 \kappa_2 c_{44}^{(1)} - \frac{\kappa_2 c_{44}^{(3)}}{c_{44}^{(4)}} \kappa_0 c_{44}^{(2)} \right] \left[u_{3,1}^{(0)} + u_{1,11}^{(1)} \right] - 4 \left[\kappa_2^2 c_{44}^{(2)} - \frac{\kappa_2 c_{44}^{(3)}}{c_{44}^{(4)}} \kappa_2 c_{44}^{(3)} \right] u_{1,11}^{(2)} \\
& = \rho^{(2)} \ddot{u}_1^{(0)} + \rho^{(3)} \ddot{u}_1^{(1)} + \rho^{(4)} \ddot{u}_1^{(2)}. \tag{12}
\end{aligned}$$

What we consider here are free vibrations. For a finite plate within $-a < x_1 < a$, the boundary conditions are

$$T_{11}^{(0)} = T_{13}^{(0)} = T_{11}^{(1)} = T_{13}^{(1)} = T_{11}^{(2)} = 0, \quad x_1 = \pm a. \tag{13}$$

III. FREE VIBRATION SOLUTION OF A FINITE PLATE

For free vibration solutions to Eqs. (8)–(12), we let

$$\begin{aligned}
u_1^{(0)} &= A_0 \sin kx_1 \exp(i\omega t), \quad u_3^{(0)} = B_0 \cos kx_1 \exp(i\omega t), \\
u_1^{(1)} &= \frac{A_1 \sin kx_1 \exp(i\omega t)}{h}, \quad u_3^{(1)} = \frac{B_1 \cos kx_1 \exp(i\omega t)}{h}, \\
u_1^{(2)} &= \frac{A_2 \sin kx_1 \exp(i\omega t)}{h^2},
\end{aligned} \tag{14}$$

where k is the wave number. ω is the frequency. A_0, A_1, A_2, B_0 and B_1 are wave amplitudes. The substitution of Eq. (14) into Eqs. (8)–(12) results in five linear homogeneous equations for the wave amplitudes which, in matrix form, can be written as

$$[C(\Omega, \xi)]_{5 \times 5} \begin{bmatrix} A_0 \\ B_0 \\ A_1 \\ B_1 \\ A_2 \end{bmatrix} = 0, \tag{15}$$

where we have introduced the following dimensionless frequency and dimensionless wave number:

$$\Omega = \omega h \sqrt{\frac{\rho^f}{c_{44}^f}}, \quad \xi = kh. \tag{16}$$

For nontrivial solutions of the wave amplitudes, the determinant of the coefficient matrix of Eq. (15) has to vanish, i.e.,

$$\det [C(\Omega, \xi)]_{5 \times 5} = 0. \tag{17}$$

Eq. (17) is a polynomial equation of degree five for ξ^2 . For a given Ω , there are five roots for ξ^2 or ξ because the sign of ξ does not matter in Eq. (14). Corresponding to each root of ξ , the nontrivial solutions of the amplitudes determine the amplitude ratios which are denoted by

$$A_0^i : B_0^i : A_1^i : B_1^i : A_2^i = 1 : \beta_0^i : \alpha_1^i : \beta_1^i : \alpha_2^i, \quad i = 1 \sim 5. \tag{18}$$

Then the general solution to Eqs. (8)–(12) can be written as

$$\begin{aligned}
u_1^{(0)} &= \sum_{i=1}^5 A_0^i \sin\left(\frac{\xi_i x_1}{h}\right) e^{i\omega t}, & u_3^{(0)} &= \sum_{i=1}^5 A_0^i \beta_0^i \cos\left(\frac{\xi_i x_1}{h}\right) e^{i\omega t}, \\
u_1^{(1)} &= \sum_{i=1}^5 \frac{A_0^i \alpha_1^i}{h} \sin\left(\frac{\xi_i x_1}{h}\right) e^{i\omega t}, & u_3^{(1)} &= \sum_{i=1}^5 \frac{A_0^i \beta_1^i}{h} \cos\left(\frac{\xi_i x_1}{h}\right) e^{i\omega t}, \\
u_1^{(2)} &= \sum_{i=1}^5 \frac{A_0^i \alpha_2^i}{h^2} \sin\left(\frac{\xi_i x_1}{h}\right) e^{i\omega t},
\end{aligned} \tag{19}$$

where A_0^i are undetermined constants. The substitution of Eq. (19) into the boundary conditions in Eq. (13) gives five linear homogeneous equations for A_0^i :

$$[D(\Omega, a/h)]_{5 \times 5} \begin{bmatrix} A_0^1 \\ A_0^2 \\ A_0^3 \\ A_0^4 \\ A_0^5 \end{bmatrix} = 0. \tag{20}$$

For nontrivial solutions of A_0^i , the determinant of the coefficient matrix of Eq. (20) has to vanish which leads to the following frequency equation:

$$\det [D(\Omega, a/h)]_{5 \times 5} = 0. \tag{21}$$

Corresponding to each frequency, the nontrivial solutions of Eq. (20) determines the mode.

IV. NUMERICAL RESULTS AND DISCUSSION

As a numerical example, we consider the FBAR in Refs. 21 and 26 whose material constants for the piezoelectric film, the silicon layer, and the electrodes are:

$$\begin{aligned}
c_{11}^f &= 20.97 \times 10^{10} \text{N/m}^2, & c_{33}^f &= 21.09 \times 10^{10} \text{N/m}^2, & c_{13}^f &= 10.51 \times 10^{10} \text{N/m}^2, \\
c_{44}^f &= 10.51 \times 10^{10} \text{N/m}^2, & \rho^f &= 5.68 \times 10^3 \text{kg/m}^3, \\
e_{31} &= -0.573 \text{C/m}^2, & e_{33} &= 1.32 \text{C/m}^2, & e_{15} &= -0.48 \text{C/m}^2, \\
\varepsilon_{11} &= 8.55 \varepsilon_0, & \varepsilon_{33} &= 10.2 \varepsilon_0, & \varepsilon_0 &= 8.854 \times 10^{-12} \text{F/m},
\end{aligned} \tag{22}$$

$$\begin{aligned}
c_{11}^s &= 16.57 \times 10^{10} \text{N/m}^2, & c_{33}^s &= c_{11}^s, & c_{13}^s &= 6.39 \times 10^{10} \text{N/m}^2, \\
c_{44}^s &= 7.956 \times 10^{10} \text{N/m}^2, & \rho^s &= 2.332 \times 10^3 \text{kg/m}^3,
\end{aligned} \tag{23}$$

and

$$\begin{aligned}
c'_{11} &= 18.6 \times 10^{10} \text{N/m}^2, & c'_{33} &= c'_{11}, & c'_{13} &= 15.7 \times 10^{10} \text{N/m}^2, \\
c'_{44} &= 4.2 \times 10^{10} \text{N/m}^2, & \rho' &= 19.3 \times 10^3 \text{kg/m}^3,
\end{aligned} \tag{24}$$

respectively. The geometric parameters are determined by

$$h^f = 15 \mu\text{m}, \quad h^s = 5 \mu\text{m}, \quad h'' = 0.2 \mu\text{m}, \quad R' = \rho' h' / (\rho^f h^f) = 0.01. \tag{25}$$

For such an FBAR, the correction factors were determined in Ref. 26 by matching the dispersion relations of the relevant coupled waves calculated from both the plate equations and the three dimensional equations.^{27,28} The detailed procedure can refer to our previous paper.²⁶ For simplicity, the factor values are directly given here:

$$\kappa_0 = 1.3116, \quad \kappa_1 = 2.2822, \quad \kappa_2 = 0.7022, \quad \kappa_3 = 1.6936. \tag{26}$$

Fig. 2 shows the dimensionless frequency $\Omega/\Omega_{\text{TE}}$ versus the plate length/thickness ratio a/h , where Ω_{TE} is the fundamental thickness-extensional frequency of an infinite plate ($a=\infty$). For the

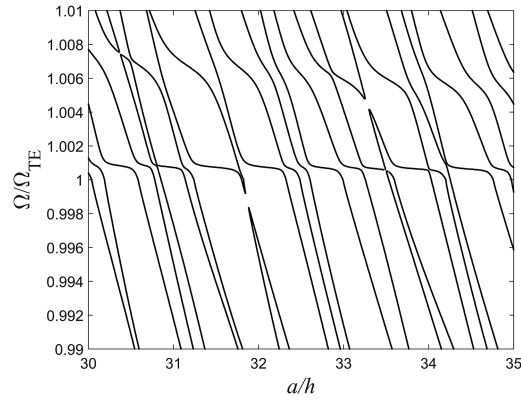


FIG. 2. FBAR frequency spectra.

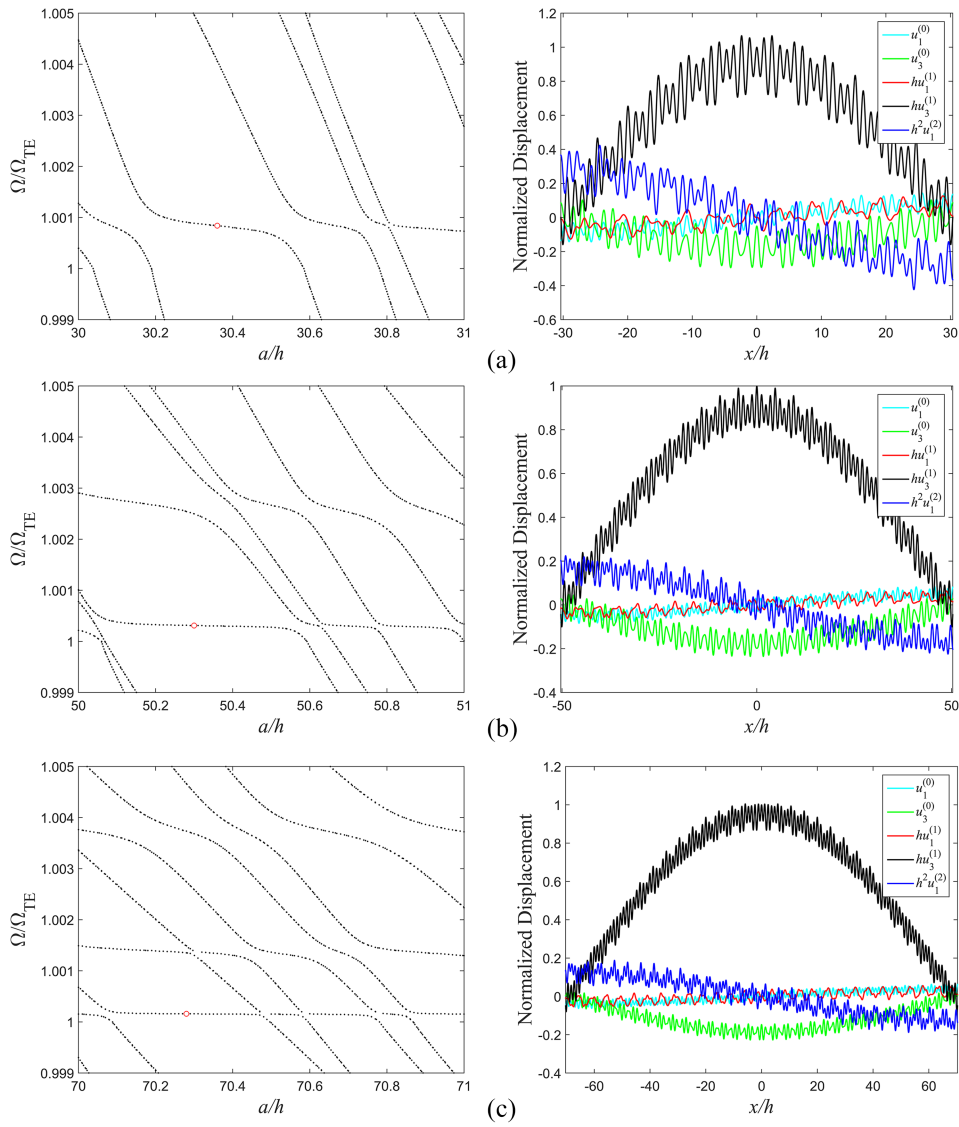


FIG. 3. Essentially thickness-extensional modes: (a) $a/h=30.36$, $\Omega/\Omega_{TE}=1.000836237$; (b) $a/h=50.30$, $\Omega/\Omega_{TE}=1.000309792$; (c) $a/h=70.28$, $\Omega/\Omega_{TE}=1.000157753$.

relatively well-studied quartz resonators, similar figures are called frequency spectra and have been systematically calculated^{29–35} because of their important applications in mode coupling analysis. The curves in Fig. 2 are in fact formed by data points close to each other without really connecting them. Each data point represents the frequency of a mode. Corresponding to a particular value of a/h , there are infinitely many modes. A few can be seen in the frequency range shown. As to be shown later in Fig. 3, the flat parts of the curves with Ω/Ω_{TE} near 1 represent the operating thickness-extensional modes with weak couplings to the other unwanted modes. When the flat parts begin to bend or seem to intersect with other curves, stronger couplings to other modes begin to occur which is undesirable in device operation and should be avoided. The usefulness of the frequency spectra is that it determines when flat parts of the curves in Fig. 1 bend or end, and thus excludes a discrete series of values of a/h .

Fig. 3 shows the plate displacement components according to Eq. (1) at the plate upper surface where $x_3=h$. They are for different values of a/h roughly in the middle of the flat parts of the curves

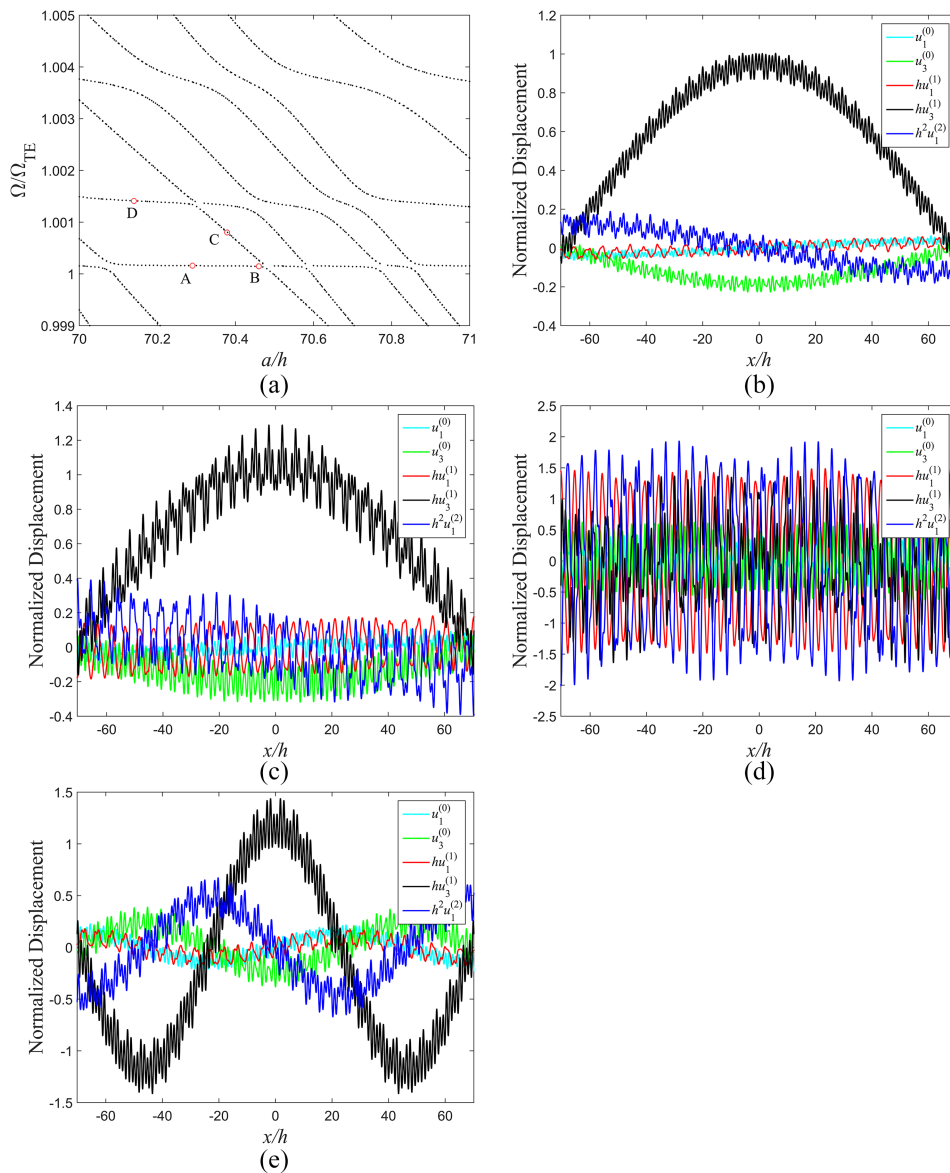


FIG. 4. A few modes within $70 < a/h < 71$: (a) Frequency spectra; (b) Point A: $a/h=70.29$, $\Omega/\Omega_{TE}=1.000157276$; (c) Point B: $a/h=70.46$, $\Omega/\Omega_{TE}=1.000144497$; (d) Point C: $a/h=70.38$, $\Omega/\Omega_{TE}=1.000800474$; (e) Point D: $a/h=70.14$, $\Omega/\Omega_{TE}=1.001412358$.

in Fig. 2 near $\Omega/\Omega_{TE}=1$. Clearly, the thickness-extensional displacement $u_3^{(1)}$ dominates in these modes and hence they are called the essentially thickness extensional modes. From (a) to (c), as a/h increases, the dominance of $u_3^{(1)}$ becomes stronger. This is because for longer plates the edge effects that cause mode couplings are less influential. Therefore, in device applications, plates with large values of a/h are with less mode couplings and are desirable as long as the requirements on size and weight allow. The frequencies of these modes decrease very slightly as a/h increases, which is as expected because the frequencies of the thickness-extensional mode are essentially determined by the plate thickness $2h$ and depend very weakly on the length $2a$, and therefore larger plates have lower frequencies.

Fig. 4 shows four modes corresponding to the four points on the curves in Fig. 4 (a). Fig. 4 (b) is for point A which is in the middle of the flat part of the curves near $\Omega/\Omega_{TE}=1$. It is an essentially thickness-extensional mode with a dominating $u_3^{(1)}$. Fig. 4 (c) is for point B which is near the end of a flat part in Fig. 4 (a). It is still thickness-extensional although $u_3^{(1)}$ is less dominating compared to Fig. 4 (b). This mode can still be used in devices but it is not as ideal as the mode in Fig. 4 (b). In Fig. 4 (d) which is for point C, no plate displacement component is dominating although the second-order thickness-shear displacement $u_1^{(2)}$ is larger than the other displacements. This mode is simply not useful for devices. The mode in Fig. 4 (e) corresponds to point D in Fig. 4 (a) which is in a flat part of the curves that is not one of those that are very close to $\Omega/\Omega_{TE}=1$. Its displacement $u_3^{(1)}$ is much larger than other displacements. However, $u_3^{(1)}$ has two nodal points (zeros) along the plate. This causes the cancellation of charges on the electrodes produced by the thickness-extensional strain through piezoelectric coupling, and, as a consequence, lowers the capacitance of the resonator which is undesirable. Therefore this mode is not useful in applications.

Fig. 5 shows a few modes with large values of a/h . The one in Fig. 5 (b) is a nice essentially thickness-extensional mode with a strongly dominating $u_3^{(1)}$. The two other modes are also essentially thickness-extensional but they correspond to the flat parts of the curves in the frequency spectra at

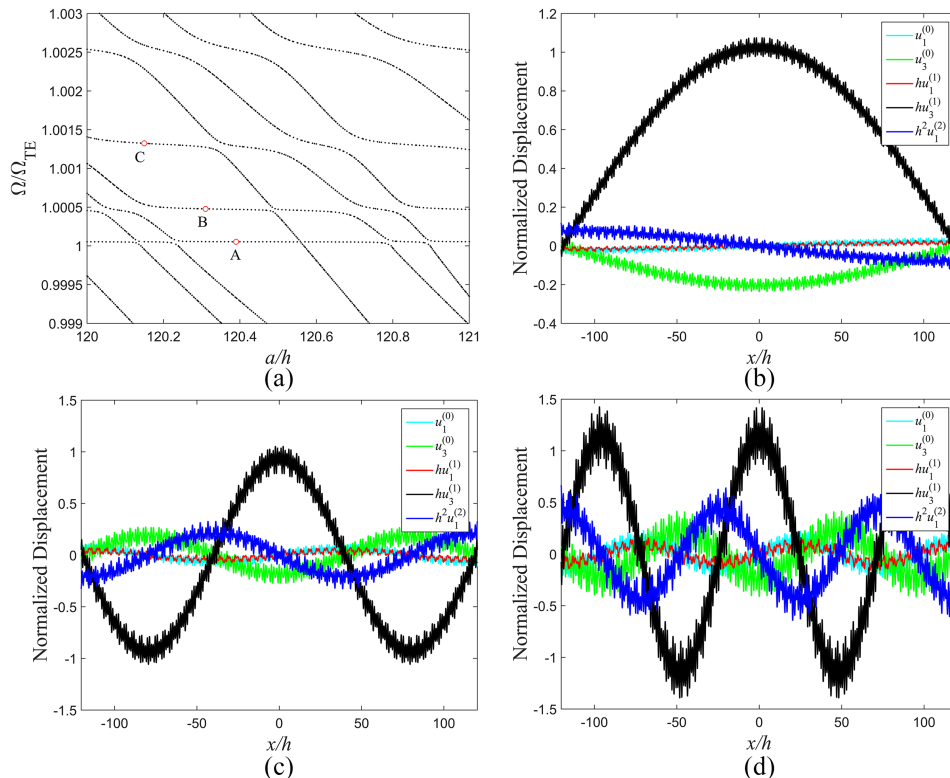


FIG. 5. A few modes within $120 < a/h < 121$: (a) Frequency spectra; (b) Point A: $a/h=120.39$, $\Omega/\Omega_{TE}=1.000053146$; (c) Point B: $a/h=120.31$, $\Omega/\Omega_{TE}=1.000477682$; (d) Point C: $a/h=120.15$, $\Omega/\Omega_{TE}=1.001323741$.

higher places. Both of these two modes have nodal points and hence the related charge cancellation as discussed after Fig. 4, and are not very useful in devices.

V. CONCLUSION

In FBARs, the operating thickness-extensional mode is coupled to the in-plane extension, flexure, fundamental and second-order thickness-shear modes. The frequency spectra obtained show that these couplings are sensitive to the plate length/thickness ratio. To avoid strong couplings to unwanted modes, a discrete series of values of the length/thickness ratio need to be avoided in design. The essentially thickness-extensional modes are more pure for plates with larger length/thickness ratios. The plate equations derived in our previous paper²⁶ are ready to be used and are effective in the modeling of mode couplings in FBARs. They can be used to produce the frequency spectra and predict when the mode coupling is weak or strong.

ACKNOWLEDGMENTS

This work was supported by the National Natural Science Foundation of China (Nos. 11502108, 11232007), the Natural Science Foundation of Jiangsu Province (No. BK20140037), the Fundamental Research Funds for Central Universities (No. NE2013101), the Program for New Century Excellent Talents in University (No. NCET-12-0625), and a project Funded by the Priority Academic Program Development of Jiangsu Higher Education Institutions (PAPD). This work was also supported by Funding of Jiangsu Innovation Program for Graduate Education (KYLX16.0312), the Fundamental Research Funds for Central Universities.

- ¹ V. E. Bottom, *Introduction to Quartz Crystal Unit Design* (Van Nostrand Reinhold, New York, 1982).
- ² D. Salt, *Quartz Crystal Devices* (Van Nostrand Reinhold, Wokingham, Berkshire, England, 1987).
- ³ C. K. Campbell, *Surface Acoustic Wave Devices for Mobile and Wireless Communications* (Academic Press, Orlando, FL, 1998).
- ⁴ K.-Y. Hashimoto, *Surface Acoustic Wave Devices in Telecommunications* (Springer, Berlin, 2000).
- ⁵ K. M. Lakin, "Thin film resonators and filters," *Proc. IEEE Ultrasonics Symp.* 1999, 895–906.
- ⁶ G. F. Iriarte, F. Engelmark, and I. V. Katardjiev, "Reactive sputter deposition of highly oriented AlN films at room temperature," *J. Mater. Res.* **17**, 1469–1475 (2002).
- ⁷ F. Martin, M.-E. Jan, S. Rey-Mermet, B. Belgacem, D. Su, M. Cantoni, and P. Muralt, "Shear mode coupling and tilted grain growth of AlN thin films in BAW resonators," *IEEE Trans. Ultrason. Ferroelectr. Freq. Control* **53**, 1339–1343 (2006).
- ⁸ K. M. Lakin, G. R. Kline, and K. T. McCarron, "Development of miniature filters for wireless applications," *IEEE Trans. Microw. Theory Tech.* **43**, 2933–2939 (1995).
- ⁹ Y. Satoh, T. Nishihara, T. Yokoyama, M. Ueda, and T. Miyashita, "Development of piezoelectric thin film resonator and its impact on future wireless communication systems," *Jpn. J. Appl. Phys., Part I* **44**, 2883–2894 (2005).
- ¹⁰ M. Link, M. Schreiter, J. Weber, R. Primig, D. Pitzer, and R. Gabl, "Solidly mounted ZnO shear mode film bulk acoustic wave resonators for sensing applications in liquids," *IEEE Trans. Ultrason. Ferroelectr. Freq. Control* **53**, 492–496 (2006).
- ¹¹ Y. Q. Fu, J. K. Luo, X. Y. Du, A. J. Flewitt, Y. Li, G. H. Markx, A. J. Walton, and W. I. Milne, "Recent developments on ZnO films for acoustic wave based bio-sensing and microfluidic applications: A review," *Sens. Actuator B-Chem.* **143**, 606–619 (2010).
- ¹² T. Yanagitani, N. Mishima, M. Matsukawa, and Y. Watanabe, "Electromechanical coupling coefficient k_{15} of polycrystalline ZnO films with the c-axis lie in the substrate plane," *IEEE Trans. Ultrason. Ferroelectr. Freq. Control* **54**, 701–704 (2007).
- ¹³ T. Yanagitani, M. Kiuchi, M. Matsukawa, and Y. Watanabe, "Characteristics of pure-shear mode BAW resonators consisting of (11 $\bar{2}$ 0) textured ZnO films," *IEEE Trans. Ultrason. Ferroelectr. Freq. Control* **54**, 1680–1686 (2007).
- ¹⁴ J. K. Du, K. Xian, J. Wang, and J. S. Yang, "Thickness vibration of piezoelectric plates of 6 mm crystals with tilted six-fold axis and two-layered thick electrodes," *Ultrasonics* **49**, 149–152 (2009).
- ¹⁵ L. F. Qin, Q. M. Chen, H. B. Cheng, and Q.-M. Wang, "Analytical study of dual-mode thin film bulk acoustic resonators (FBARs) based on ZnO and AlN films with tilted c-axis orientation," *IEEE Trans. Ultrason. Ferroelectr. Freq. Control* **57**, 1840–1853 (2010).
- ¹⁶ T. Yanagitani, N. Morisato, S. Takayanagi, M. Matsukawa, and Y. Watanabe, "C-axis zig-zag ZnO film ultrasonic transducers for designing longitudinal and shear wave resonant frequencies and modes," *IEEE Trans. Ultrason. Ferroelectr. Freq. Control* **58**, 1062–1068 (2011).
- ¹⁷ S.-H. Lee, K. H. Yoon, and J.-K. Lee, "Influence of electrode configurations on the quality factor and piezoelectric coupling constant of solidly mounted bulk acoustic wave resonators," *J. Appl. Phys.* **92**, 4062–4069 (2002).
- ¹⁸ Y. F. Zhang and D. Chen, *Multilayer Integrated Film Bulk Acoustic Resonators* (Shanghai Jiaotong University Press, Shanghai, 2013).
- ¹⁹ E. Milyutin and P. Muralt, "Electro-mechanical coupling in shear-mode FBAR with piezoelectric modulated thin film," *IEEE Trans. Ultrason. Ferroelectr. Freq. Control* **58**, 685–688 (2011).
- ²⁰ H. F. Zhang and J. A. Kosinski, "Analysis of thickness vibrations of c-axis inclined z-g-zag two-layered zinc oxide thin-film resonators," *IEEE Trans. Ultrason. Ferroelectr. Freq. Control* **59**, 2831–2836 (2012).

- ²¹ H. F. Tiersten and D. S. Stevens, "An analysis of thickness-extensional trapped energy resonant device structures with rectangular electrodes in the piezoelectric thin film on silicon configuration," *J. Appl. Phys.* **54**, 5893–5910 (1983).
- ²² Z. N. Zhao, Z. H. Qian, B. Wang, and J. S. Yang, "Energy trapping of thickness-extensional modes in thin film bulk acoustic wave resonators," *J. Mech. Sci. Technol.* **29**(7), 2767–2773 (2015).
- ²³ Z. N. Zhao, Z. H. Qian, and B. Wang, "Energy trapping of thickness-extensional modes in thin film bulk acoustic wave filters," *AIP Adv.* **6**(1), 015002 (2016).
- ²⁴ Z. N. Zhao, Z. H. Qian, and B. Wang, "Vibration optimization of ZnO thin film bulk acoustic resonator with ring electrodes," *AIP Adv.* **6**(4), 1735–1739 (2016).
- ²⁵ J. Wang, R. X. Wu, L. J. Yang, J. K. Du, and T. F. Ma, "The fifth-order overtone vibrations of quartz crystal plates with corrected higher-order Mindlin plate equations," *IEEE Trans. Ultrason. Ferroelectr. Freq. Control* **59**(10), 2278–2291 (2012).
- ²⁶ N. Li, Z. H. Qian, and J. S. Yang, "Two-dimensional equations for piezoelectric thin-film acoustic wave resonators," *Int. J. Solids Struct.* **110**, 170–177 (2017).
- ²⁷ F. Zhu, Z.-h. Qian, and B. Wang, "Wave propagation in piezoelectric layered structures of film bulk acoustic resonators," *Ultrasonics* **67**, 105–111 (2016).
- ²⁸ H. Chen, J. Wang, J. K. Du, and J. S. Yang, "Shear-horizontal piezoelectric waves in an aluminum nitride film on a silicon substrate," *Mech. Adv. Mater. Struct.* **23**(7), 764–773 (2016).
- ²⁹ R. D. Mindlin, "High frequency vibrations of piezoelectric crystal plates," *Int. J. Solids Struct.* **8**, 895–906 (1972).
- ³⁰ P. C. Y. Lee, S. Syngellakis, and J. P. Hou, "A two-dimensional theory for high-frequency vibrations of piezoelectric crystal plates with or without electrodes," *J. Appl. Phys.* **61**(4), 1249–1262 (1987).
- ³¹ J. Wang, Y.-K. Yong, and T. Imai, "A new theory for electroded piezoelectric plates and its finite element application for the forced vibrations of quartz crystal resonators," *Int. J. Solids Struct.* **37**, 5653–5673 (2000).
- ³² J. Wang, Y.-K. Yong, and T. Imai, "Finite element analysis of the piezoelectric vibrations of quartz plate resonators with higher-order plate theory," *Int. J. Solids Struct.* **36**(15), 2303–2319 (1999).
- ³³ J. N. Wang, Y. T. Hu, and J. S. Yang, "Frequency spectra of AT-cut quartz plates with electrodes of unequal thickness," *IEEE Trans. Ultrason., Ferroelectr., Freq. Contr.* **57**(5), 1146–1151 (2010).
- ³⁴ G. J. Chen, R. X. Wu, J. Wang, J. K. Du, and J. S. Yang, "Five-mode frequency spectra of x_3 -dependent modes in AT-cut quartz resonators," *IEEE Trans. Ultrason., Ferroelectr., Freq. Contr.* **59**(4), 811–816 (2012).
- ³⁵ J. Zhu, W. Q. Chen, and J. S. Yang, "Overtone frequency spectra for x_3 -dependent modes in AT-cut quartz resonators," *IEEE Trans. Ultrason., Ferroelectr., Freq. Contr.* **60**(4), 858–863 (2013).